

# Formulation of geopotential difference determination using optical-atomic clocks onboard satellites and on ground based on Doppler cancellation system

Ziyu Shen,<sup>1</sup> Wen-Bin Shen<sup>1,2</sup> and Shuangxi Zhang<sup>1</sup>

<sup>1</sup>*Department of Geophysics, School of Geodesy and Geomatics, Wuhan University, Wuhan 430079, China*

<sup>2</sup>*State Key Laboratory of Information Engineering in Surveying, Mapping and Remote Sensing, Wuhan University, Wuhan 430079, China. E-mail: wbsen@sgg.whu.edu.cn*

Accepted 2016 May 19. Received 2016 May 18; in original form 2016 February 14

## SUMMARY

In this study, we propose an approach for determining the geopotential difference using high-frequency-stability microwave links between satellite and ground station based on Doppler cancellation system. Suppose a satellite and a ground station are equipped with precise optical-atomic clocks (OACs) and oscillators. The ground oscillator emits a signal with frequency  $f_a$  towards the satellite and the satellite receiver (connected with the satellite oscillator) receives this signal with frequency  $f_b$  which contains the gravitational frequency shift effect and other signals and noises. After receiving this signal, the satellite oscillator transmits and emits, respectively, two signals with frequencies  $f_b$  and  $f_c$  towards the ground station. Via Doppler cancellation technique, the geopotential difference between the satellite and the ground station can be determined based on gravitational frequency shift equation by a combination of these three frequencies. For arbitrary two stations on ground, based on similar procedures as described above, we may determine the geopotential difference between these two stations via a satellite. Our analysis shows that the accuracy can reach  $1 \text{ m}^2 \text{ s}^{-2}$  based on the clocks' inaccuracy of about  $10^{-17} \text{ (s s}^{-1}\text{)}$  level. Since OACs with instability around  $10^{-18}$  in several hours and inaccuracy around  $10^{-18}$  level have been generated in laboratory, the proposed approach may have prospective applications in geoscience, and especially, based on this approach a unified world height system could be realized with one-centimetre level accuracy in the near future.

**Key words:** Satellite gravity; Geopotential theory; Ionosphere/atmosphere interactions.

## 1 INTRODUCTION

One of the main objectives in geodesy is to accurately determine the geopotential as well as the orthometric height. If the geopotential can be precisely determined, then the orthometric height can be accordingly precisely determined (Hofmann-Wellenhof & Moritz 2006). Another objective is to unify the world height datum system with high accuracy. The conventional approach of determining the geopotential (as well as the orthometric height) by combining levelling and gravimetry has at least the following two drawbacks: (1) the error is accumulated with the increase of the length of the measurement line, and (2) it is difficult or impossible to transfer the orthometric height with high accuracy between two points located in mountainous areas or continents separated by sea. The point (2) of the drawbacks also means that it is very difficult to unify the

world height datum system with high accuracy, which is an open problem in geodetic community.

In recent decades, though gravity field models (such as GOCE/GRACE geopotential models and EGM2008 models) can be used for determining geopotential, there exist essential limitations. For instance, the main problems existing in the GRACE-generated gravity field or GOCE-generated gravity field are that their resolution is low, achieving about  $2^\circ \times 2^\circ$  to  $1^\circ \times 1^\circ$ , equivalent to about 200–100 km resolution (Tapley *et al.* 2004; Pail *et al.* 2011). At present, though the gravity field model EGM2008 with degree/order 2160 (Pavlis *et al.* 2008) has the highest accuracy and resolution (about 10 km), its average accuracy is around 10–20 cm, which is not enough for high precision requirement (say several centimetres). In addition, it provides only 'average' results, not *in situ*. To overcome the difficulties existing in conventional approach

for determining the geopotential difference, Bjerhammar (1985) put forward an idea to determine the gravitational potential using clock transportation approach (Shen *et al.* 2009), which is based on the general relativity theory (Einstein 1915). The geopotential difference is determined by precise clocks, since clocks run at different rates at the positions with different geopotentials according to general theory of relativity. Equivalently, Shen *et al.* (1993) suggested that the gravitational potential could be determined by gravity frequency shift, because light signal's frequency will change as it travels between two positions with different geopotentials. In addition, Shen *et al.* (1993, 2011) proposed an approach, which stated that the geopotential could be determined by satellite frequency signal transmission, which may play a key role in directly determining the geopotential and unifying the world height datum system. This method is prospective and potential to be applied in the Global Navigation Satellite System (GNSS; Shen *et al.* 1993, 2011), since GNSS satellites almost cover every corner of the Earth's surface.

The principle of determining geopotential difference via GNSS frequency signals was introduced in our previous studies (Shen *et al.* 1993, 2011). However, a key problem open is how to effectively extract gravitational frequency shift from various frequency shifts caused by other sources, such as Doppler frequency shift, ionospheric influence, etc. In this paper, we propose an approach to extract gravitational frequency shift from the propagation of light signals between a spacecraft (space station or satellite) and a ground station based on Doppler cancelling technique (DCT; Vessot & Levine 1979) which was proposed to test the general relativity theory. By extracting the gravitational frequency shift signals between the spacecraft and the ground station, we can determine the geopotential difference. Since optical-atomic clocks (OACs) with instability around  $10^{-18}$  ( $\text{s}^{-1}$  or  $\text{Hz Hz}^{-1}$ ) in several hours and inaccuracy of  $10^{-18}$  level have been generated in laboratory (Hinkley *et al.* 2013; Bloom *et al.* 2014; Ushijima *et al.* 2015), we may expect that in the very near future, portable or commercial clocks with inaccuracy of  $10^{-18}$  level could be generated. For instance, the project Space Optical Clocks 2 of European Space Agency planned to install transportable lattice optical clocks with inaccuracy of  $10^{-16}$ – $10^{-17}$  on board (Schiller *et al.* 2012; Botter *et al.* 2014). The Space-Time Explorer and QUantum Equivalence Space Test space mission was planned to be launched around 2024 which can compare clocks between satellite and ground down to the inaccuracy of  $1 \times 10^{-18}$  level (Altschul *et al.* 2014; Hechenblaikner *et al.* 2014). China planned to launch Experiment Space Station in the period 2021–2023, in which an OAC system with inaccuracy of  $10^{-17}$  level or better will be installed on board (Private communication, 2015). The main purposes that ultrahigh precision clocks are installed in a Space Station include not only further testing general relativity theory but also investigating broad applications of ultrahigh precise time–frequency systems. Thus, the proposed approach in this study is prospective for precisely determining the geopotential globally. Further, based on this approach a unified world height system could be realized with high accuracy. In this study, we assume that the clocks with relative inaccuracy of  $1 \times 10^{-17}$  level are available in the near future.

Although the gravitational potential changes as a function of time, due to mass migration for instance associated with tides, ice melting, sea level rise and so on, here we deal with static geopotential measurements. The corrections from temporal to static fields are well known, an inspection beyond the scope of this study. In fact, we determine the difference between the geopotential  $W_S(t)$  of the satellite-orbit position at some point in time  $t$  and the fixed geopotential  $W_A$  at the ground station (see Fig. 1).

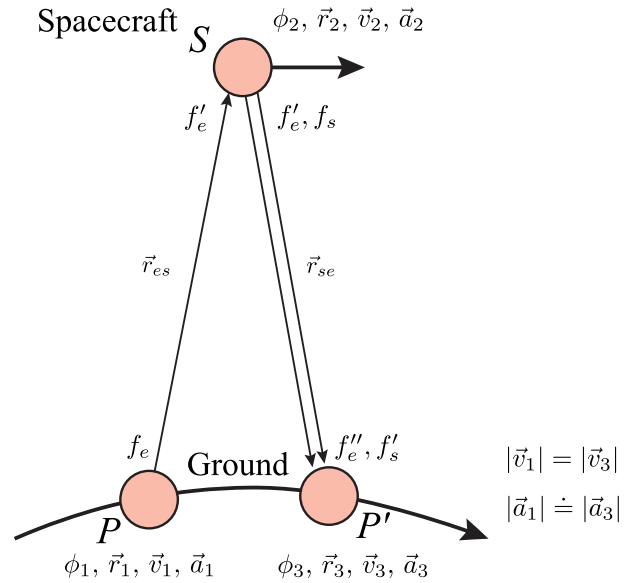


**Figure 1.** Ground station  $P$  emits a frequency signal  $f_e$  at time  $t_1$ . Satellite  $S$  transmits the received signal  $f'_e$  and emits a frequency signal  $f_s$  at time  $t_2$ . The ground station receives signal  $f''_e$  and  $f'_s$  at time  $t_3$  at position  $P'$ .  $\phi$  is gravitational potential,  $\vec{r}$  is position vector,  $\vec{v}$  is velocity vector and  $\vec{a}$  is centrifugal acceleration vector.

## 2 DOPPLER CANCELLING TECHNIQUE

When a frequency signal is emitted from satellite to ground or from ground station to satellite, the first-order Doppler effect contributes the most amount of frequency shift. However, the first-order Doppler effect is hard to be precisely measured due to the fact that the velocity of satellite cannot be precisely enough determined. Thus, the gravity frequency shift cannot effectively be identified if the first-order Doppler effect is not cancelled. Fortunately, this problem could be solved by using the DCT (Vessot & Levine 1979). After the first-order Doppler effects are eliminated, the remained frequency shift effects caused by other factors are more easily to be distinguished. After subtracting the ionosphere frequency shift, troposphere frequency shift and other influences, we can obtain the target gravity frequency shift. In fact, the DCT not only cancels the first-order Doppler effect, but also almost eliminates the ionosphere and troposphere effects.

The DCT (Vessot & Levine 1979) contains three micro-wave links as depicted in Fig. 1. Ground station  $P$  emits a frequency signal  $f_e$  at time  $t_1$ . When the signal is received by satellite  $S$  at time  $t_2$ , it immediately transmits the received signal  $f'_e$  and emits a frequency signal  $f_s$  at the same time. These two signals emitted from satellite are received by ground station  $P$  at time  $t_3$ , noting that during the time period from  $t_1$  to  $t_3$  the ground station has changed from position  $P$  to position  $P'$ .

As described in Fig. 1, we can extract the gravity frequency shift signals (or equivalently gravitational frequency shift signals) by combining the emitting and receiving frequencies. The simplest case is when  $f_e = f_s$ , the frequency shift signals can be determined (referring to Fig. 2). The frequencies of the signals emitted from ground oscillator and satellite oscillator are  $f_0$ . The microwave links 1 and 2 consist of a go-return link by a phase-coherent microwave transponder equipped at satellite, and provide two-way Doppler frequency shift data as a beat frequency  $f''_0 - f_0$  (Vessot & Levine 1979). Similarly, the microwave link 3 provides one-way frequency shift data as a beat frequency  $f'_0 - f_0$  (Vessot & Levine 1979). Dividing the two-way beat frequency by two and subtracting it

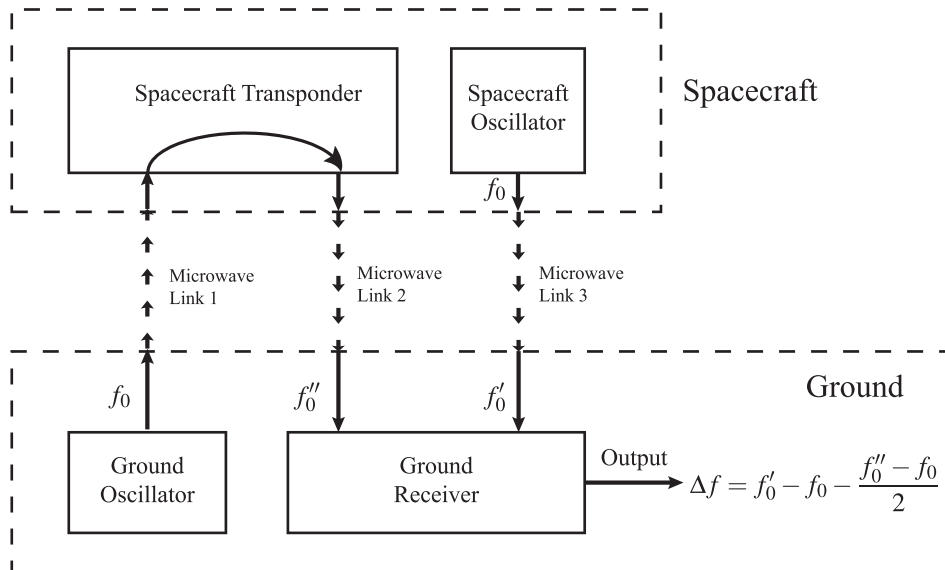


**Figure 2.** Schematic concept of the Doppler cancelling system (modified after Vessot & Levine 1979). The ground oscillator emits a frequency signal  $f_0$  to the spacecraft, then the spacecraft transmits the received signal to ground, and emits a frequency signal  $f_0$  from spacecraft oscillator to the ground at the same time. The signals that are transmitted and emitted from satellite are received at ground station as  $f_0'$  and  $f_0''$ , respectively. Finally, the output signal  $\Delta f$  are calculated from  $f_0'$ ,  $f_0'$  and  $f_0''$ , as described in the text (see Section 2).

from the one-way beat frequency, we obtain the equation of output frequency  $\Delta f$  (Vessot & Levine 1979):

$$\Delta f = f_0' - f_0 - \frac{f_0'' - f_0}{2}. \quad (1)$$

If the clock errors and the errors introduced during the signals' propagation (such as ionosphere influence, random noises, etc.) are neglected, the beat frequencies  $f_0' - f_0$  and  $f_0'' - f_0$  mainly consist of first-order Doppler effects, second-order Doppler effects and gravitational effect (conventionally referred to as gravitational red shift). After the subtraction of the two beat frequencies, the first-order Doppler effect is removed and the second-order Doppler effect can be calculated. Although this subtraction cannot totally cancel out the first-order Doppler effect because of Earth's rotation, we can manage to make additional correction for it. Then, we may obtain the gravitational red shift, and consequently, the gravitational potential difference.

In an ideal case, in an Earth-centred inertial coordinate system the output frequency  $\Delta f$  can be expressed as following equation (Vessot & Levine 1979)

$$\frac{\Delta f}{f_0} = \frac{\phi_s - \phi_e}{c^2} - \frac{|\vec{v}_e - \vec{v}_s|^2}{2c^2} - \frac{\vec{r}_{se} \cdot \vec{a}_e}{c^2}, \quad (2)$$

where  $\phi_s - \phi_e$  is Newtonian gravitational potential difference between ground station and spacecraft (satellite),  $\vec{v}_e$  and  $\vec{v}_s$  are velocities of ground station and spacecraft respectively,  $\vec{r}_{se}$  is vector from spacecraft to ground station,  $\vec{a}_e$  is centrifugal acceleration vector of ground station and  $c$  is the speed of light in vacuum. We note that, on the right-hand side of eq. (2), the first term denotes the gravitational red shift, the second term is identified as the second-order Doppler shift predicted by special relativity and the third term describes the effect of Earth's rotation during the propagation time  $|\vec{r}_{se}|/c$  of the light signal. It serves as an Earth's rotation correction term for the Doppler effect. Though this correction is quite small, around  $10^{-16}$ , it should be taken into account for the accuracy requirement of  $10^{-17}$  level.

Eq. (2) describes an ideal case for the DCT. However, a signals' frequency will be influenced by ionospheric and tropospheric effects (Millman & Arabadjis 1984). Similar to Doppler effect, these influences cannot be totally cancelled out in eq. (1) because of Earth's rotation. Besides, various error sources should also be considered. Thus, the output frequency  $\Delta f$  should be expressed as

$$\frac{\Delta f}{f_0} = \frac{\phi_s - \phi_e}{c^2} - \frac{|\vec{v}_e - \vec{v}_s|^2}{2c^2} - \frac{\vec{r}_{se} \cdot \vec{a}_e}{c^2} + \frac{\Delta f_i}{f_0} + \frac{\Delta f_t}{f_0} + \frac{\Delta f_e}{f_0}, \quad (3)$$

where  $\Delta f_i$  is ionospheric shift correction term (see Section 3.1),  $\Delta f_t$  is troposphere refraction effect correction term (see Section 3.2),  $\Delta f_e$  is the error term which contain clock error, position error, velocity error, instrumental error, remained ionospheric shift error, remained tropospheric effect error and random errors. The clock error reflects the stability of oscillator, and the instrumental error contains a finite delay in spacecraft transponder. Since the DCT method only involves frequency measurement, it does not require time synchronization or calibration. Thus, the hardware delays in ground station can be neglected, if there is any.

Here, we only focus on determining the geopotential difference between a satellite/spacecraft and a ground station, which means that the absolute value of the geopotential at the satellite/spacecraft's orbit is not considered in this study. For the determination of the absolute geopotential at a ground station via a satellite/spacecraft, the absolute value of the geopotential at the satellite/spacecraft's orbit should be *a priori* given. The determination of the geopotential difference between two ground stations can be realized via satellite frequency signal links. The determination of the (absolute) geopotential at a ground station and inversely that at satellite position at time  $t$  are topics of our future research. In the sequel, we will discuss the correction terms  $\Delta f_i$  and  $\Delta f_t$  in details.

### 3 IONOSPHERE AND TROPOSPHERE CORRECTION

#### 3.1 Ionospheric shift correction

When a microwave signal travels through ionosphere, the Doppler and ionospheric frequency shift  $\Delta f$  is caused by the time variation of the phase path  $P$  (Namazov *et al.* 1975):

$$\Delta f = -\frac{f}{c} \frac{dP}{dt} \quad (4)$$

and the phase path  $P$  in ionosphere can be expressed as:

$$P = \int_L n_i ds \quad (5)$$

where  $n_i$  is the refractive index of ionosphere and  $L$  is the path of the signal's propagation. The refractive index  $n_i$  in ionosphere is described as (Vessot & Levine 1979):

$$n_i = \left( 1 - \frac{f_n^2}{f^2 [1 \pm (f_m/f)]} \right)^{1/2}, \quad (6)$$

where  $f_n$  is plasma frequency and  $f_m$  is electron gyromagnetic frequency. The plasma frequency is described as

$$f_n = \frac{1}{2\pi} \left( \frac{\rho}{\epsilon_0 m} e^2 \right)^{1/2} \quad (7)$$

where  $e$  and  $m$  are electron's charge and mass,  $\rho$  is density (electron number per cubic metre) and  $\epsilon_0$  is the permittivity of free space. When  $f = 2.0$  GHz, the term  $f_m/f \approx 3 \times 10^{-3}$  can be neglected. Combining eqs (4)–(7), we have

$$\Delta f = -\frac{f}{c} \frac{d}{dt} \int_L n_i ds = -\frac{f}{c} \frac{d}{dt} \int_L ds + \frac{40.5}{cf} \frac{d}{dt} \int_L \rho(t) ds \quad (8)$$

where in the right-hand side, the first term represents the conventional Doppler shift, and the second term represents the ionospheric influence. The first Doppler effect can be completely cancelled after application of DCT. Hence, the interested ionospheric shift can be expressed as

$$\Delta f_i = \frac{40.5}{cf} \frac{d}{dt} \int_L \rho(t) ds \quad (9)$$

where  $\int_L \rho(t) ds$  is the columnar electron density, and from eq. (9) we can see that the ionosphere frequency shift  $\Delta f_i$  may be caused by the variation of electron density  $\rho$  along the trajectory and by the variation of the geometric path of the signal.

Eq. (9) describes the ionosphere frequency shift for a single wave link. However, our DCT contains a two-way go-return link and a single downlink as shown in Fig. 2. The uplink and downlink paths are different due to the Earth's rotation, thus the uplink wave path  $l_{i1}$  in ionosphere is slightly different from the downlink wave path  $l_{i2}$  in ionosphere, as shown in Fig. 3. Based on eq. (9), the ionosphere frequency shift  $\Delta f_{ud}$  of go-return (i.e. up- and down-) link is:

$$\Delta f_{ud} = \frac{40.5}{cf} \frac{d}{dt} \left( \int_{l_{i1}} \rho ds + \int_{l_{i2}} \rho ds \right) \quad (10)$$

while the ionosphere frequency shift  $\Delta f_d$  of downlink is:

$$\Delta f_d = \frac{40.5}{cf} \frac{d}{dt} \int_{l_{i2}} \rho ds. \quad (11)$$

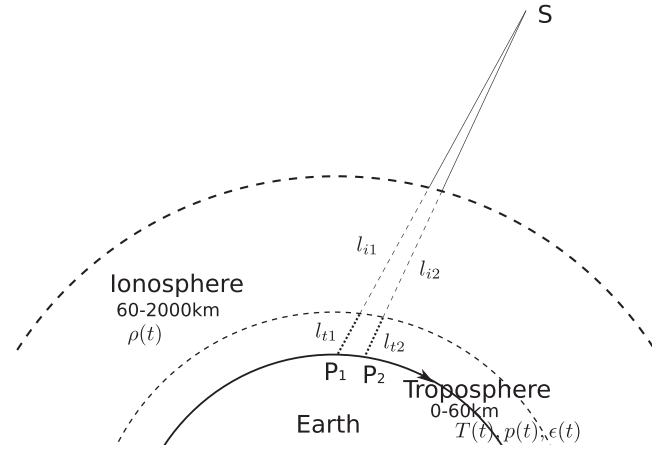


**Figure 3.** The path difference between uplink and downlink. The oscillator at ground station emits a frequency signal at point  $P_1$ , then the spacecraft (satellite) at  $S$  receives and transmits the signal toward the ground station. Finally, the receiver at ground station receives the transmitted signal at point  $P_2$  because of Earth's rotation.  $l_{i1}$  and  $l_{i2}$  are the uplink and downlink wave paths in ionosphere respectively,  $l_{t1}$  and  $l_{t2}$  are the uplink and downlink wave paths in troposphere, respectively.

Considering the output frequency defined by eq. (1), the frequency shift  $\Delta f_i$  caused by ionosphere frequency effect in output frequency is:

$$\Delta f_i = \Delta f_d - \frac{\Delta f_{ud}}{2} = \frac{40.5}{2cf} \frac{d}{dt} \left( \int_{l_{i2}} \rho ds - \int_{l_{i1}} \rho ds \right). \quad (12)$$

#### 3.2 Tropospheric refraction effect correction

When a microwave signal travels through troposphere, similar to the ionospheric case, we have the tropospheric frequency shift equation (Millman & Arabadjis 1984):

$$\Delta f = -\frac{f}{c} \frac{d}{dt} \int_L n_t ds \quad (13)$$

where  $n_t$  is the refractive index of troposphere, which is expressed as (Millman & Arabadjis 1984):

$$n_t = 1 + \frac{a}{T} \left( p + \frac{b\epsilon}{T} \right) \times 10^{-6}, \quad (14)$$

where  $T$  is absolute temperature ( $^{\circ}\text{K}$ ),  $p$  is total pressure (mbar) and  $\epsilon$  is the partial pressure of water vapour (mbar),  $a$  and  $b$  are constants, with their values being  $77.6 \text{ K mbar}^{-1}$  and  $4810 \text{ K}$ , respectively (Smith & Weintraub 1953). According to eqs (13) and (14), similar to the ionospheric case (omitting the first Doppler term), we obtain the troposphere shift, expressed as

$$\Delta f_t = -\frac{f}{c} \frac{d}{dt} \int_L (M_1 + M_2) ds \quad (15)$$

where  $M_1 = 77.6 \times 10^{-6} p/T$  and  $M_2 = 0.373\epsilon/T^2$ . From eq. (15), we can see that the troposphere frequency shift  $\Delta f_t$  may be caused by the variation of temperature  $T$ , total pressure  $p$  and partial pressure of water vapour  $\epsilon$  along the trajectory, or by the variation of the geometric path of the signal.

Similar to eq. (12) that describes the frequency shift caused by the ionosphere effect, the frequency shift  $\Delta f_t$  caused by troposphere refraction effect in output frequency is

$$\Delta f_t = -\frac{f}{2c} \frac{d}{dt} \left( \int_{l_{i2}} (M_1 + M_2) ds - \int_{l_{i1}} (M_1 + M_2) ds \right). \quad (16)$$

### 3.3 Simplified expressions for ionosphere and troposphere correction

In previous subsections, we derived eqs (12) and (16) as the expressions for ionospheric and tropospheric frequency shift corrections, which can be used in practice. However, for convenience in practical usage in calculating the relevant quantity and estimating the accuracy, we can further simplify eqs (12) and (16) as described in the sequel.

The signal propagation paths  $l_{i1}$  and  $l_{i2}$  (in ionosphere) are relatively close to each other (Fig. 3), thus it is safe to ignore the difference of the electron density  $\rho$  between the paths  $l_{i1}$  and  $l_{i2}$ . Then, the ionospheric frequency correction  $\Delta f_i$  is only caused by variations of the geometric path of the wave, and eq. (12) can be expressed as:

$$\Delta f_i = \frac{40.5\bar{\rho}}{2cf} \left( \frac{dl_{i2}}{dt} - \frac{dl_{i1}}{dt} \right) = \frac{40.5\bar{\rho}}{2cf} (|\vec{v}_{i2}| - |\vec{v}_{i1}|), \quad (17)$$

where  $\vec{v}_{i1}$  and  $\vec{v}_{i2}$  denote the variation velocities of  $\vec{l}_{i1}$  and  $\vec{l}_{i2}$  (see Fig. 3) (here  $\vec{l}_{ij}$  denote the vector from ground station to satellite at time  $t_j, j = 1, 2$ ),  $\bar{\rho}$  is the average electron density along the signals' propagation paths  $l_{i1}$  and  $l_{i2}$ .

The signal propagation paths  $l_{t1}$  and  $l_{t2}$  (in troposphere) are very similar to the case in ionosphere, hence we can also ignore the difference of  $M_1$  and  $M_2$  between the paths  $l_{t1}$  and  $l_{t2}$ . Then, eq. (16) can be expressed as:

$$\Delta f_t = -\frac{f(\bar{M}_1 + \bar{M}_2)}{2c} (|\vec{v}_{t2}| - |\vec{v}_{t1}|), \quad (18)$$

where  $\vec{v}_{t1}$  and  $\vec{v}_{t2}$  denote the variation velocities of  $\vec{l}_{t1}$  and  $\vec{l}_{t2}$  (here  $\vec{l}_{ij}$  denote the vector from ground station to satellite at time  $t_j, j = 1, 2$ ),  $\bar{M}_1$  and  $\bar{M}_2$  are the average value of  $M_1$  and  $M_2$  along the signals' propagation paths  $l_{t1}$  and  $l_{t2}$ .

The uplink and downlink paths between ground station and spacecraft are, respectively, denoted as  $P_1S$  and  $P_2S$ , as shown by Fig. 3. We define the variation velocities of paths  $P_1S$  and  $P_2S$  as  $\vec{V}_1$  and  $\vec{V}_2$ , respectively, then we have the following relationship (note that  $|\vec{a}_e| \cdot \Delta t$  is much smaller than  $|\vec{v}_s - \vec{v}_e|$ ):

$$\begin{aligned} |\vec{V}_2| - |\vec{V}_1| &= |\vec{v}_s - \vec{v}_e - \vec{a}_e \cdot \Delta t| - |\vec{v}_s - \vec{v}_e| \\ &= |\vec{a}_e| \cdot \Delta t \cdot \cos\alpha \\ &= \vec{a}_e \cdot \frac{2|\vec{r}_{se}|}{c} \cdot \frac{(\vec{v}_s - \vec{v}_e) \cdot \vec{a}_e}{|\vec{v}_s - \vec{v}_e| |\vec{a}_e|} \\ &= \frac{2|\vec{r}_{se}| \cdot (\vec{v}_s - \vec{v}_e) \cdot \vec{a}_e}{c \cdot |\vec{v}_s - \vec{v}_e|}, \end{aligned} \quad (19)$$

where  $\vec{v}_s$  and  $\vec{v}_e$  are velocities of spacecraft and ground station, respectively,  $\vec{a}_e$  is centripetal acceleration of ground station,  $\vec{r}_{se}$  is vector from spacecraft to ground station,  $\alpha$  is the angle between relative velocity  $\vec{v}_s - \vec{v}_e$  and acceleration  $\vec{a}_e$ ,  $\Delta t$  is the time duration of go-return microwave link. Suppose the height of the spacecraft is  $H$  (km) from the ground, then we have the following approximations:

$$\begin{aligned} |\vec{v}_{i2}| - |\vec{v}_{i1}| &\approx \frac{1940}{H} (|\vec{V}_2| - |\vec{V}_1|) \\ |\vec{v}_{t2}| - |\vec{v}_{t1}| &\approx \frac{60}{H} (|\vec{V}_2| - |\vec{V}_1|), \end{aligned} \quad (20)$$

where 1940 (km) and 60 (km) denote the thicknesses of ionosphere and troposphere layers, respectively. According to eqs (17) and (18),

the ionospheric and tropospheric frequency correction terms  $\Delta f_i$  and  $\Delta f_t$  can be, respectively, written as

$$\Delta f_i = \frac{78570\bar{\rho} |\vec{r}_{se}| (\vec{v}_s - \vec{v}_e) \cdot \vec{a}_e}{c^2 f H |\vec{v}_s - \vec{v}_e|} \quad (21)$$

and

$$\Delta f_t = -\frac{60f (\bar{M}_1 + \bar{M}_2) |\vec{r}_{se}| (\vec{v}_s - \vec{v}_e) \cdot \vec{a}_e}{c^2 H |\vec{v}_s - \vec{v}_e|}. \quad (22)$$

In the above, we have discussed in detail a microwave signal's frequency shift caused by ionosphere and troposphere. It should be noted that, according to our DCT concept described in Section 2, what we need to measure are frequencies, not time duration. Besides, the delay of a microwave signal do not influence its frequency shift [see eqs (4) and (13), there are no terms describing signal's delay]. Thus, the influences caused by the ionosphere and troposphere delays are not our interests. The main frequency shift error sources caused by ionosphere and troposphere are ionospheric and tropospheric Doppler effects, just as discussed in details in Sections 3.1 and 3.2. Since we have made corrections for the ionospheric and tropospheric Doppler effects [see eqs (21) and (22)], and the remained errors are at the level of  $10^{-19}$  after corrections [see eqs (29) and (30)]. Thus, after corrections as given by eqs (21) and (22), the frequency shift errors caused by ionosphere and troposphere can be neglected.

## 4 ACCURACY ESTIMATION AND ERROR ANALYSIS

After the ionospheric and tropospheric frequency corrections [see eqs (21) and (22)], the remained error term  $\Delta f_e$  in eq. (3) is a sum of various error sources, expressed as

$$\Delta f_e = \Delta f_{\text{osc}} + \Delta f_{\text{pos}} + \Delta f_{\text{vel}} + \Delta f_{\text{rion}} + \Delta f_{\text{rtro}} + \Delta f_{\text{ran}} \quad (23)$$

where  $\Delta f_{\text{osc}}$  is oscillator error,  $\Delta f_{\text{pos}}$  is position error,  $\Delta f_{\text{vel}}$  is velocity error,  $\Delta f_{\text{rion}}$  is the residual ionosphere frequency shift error,  $\Delta f_{\text{rtro}}$  is the residual troposphere frequency shift error,  $\Delta f_{\text{ran}}$  is the sum of instrumental errors, other high-order errors and random errors.

To estimate the quantity of  $\Delta f_e$  in a realistic DCT, we assume that the spacecraft is a typical GNSS satellite whose average height is about 20 000 km above the ground (Cohenour & Graas 2011), and the satellite and ground station are both equipped with OACs with inaccuracy of  $10^{-17}$  (Westergaard *et al.* 2011). The frequency  $f_0$  of the signals used is assumed as 2.0 GHz (Levine 2008).

In this study we assume that OACs with their inaccuracy about  $1 \times 10^{-17}$  are available. Hence, we have  $\Delta f_{\text{osc}}/f_0 = 1 \times 10^{-17}$ . The distance between satellite and ground station,  $|\vec{r}_{se}|$ , is around 22 000 km (the angle between observation sight and zenith is within  $35^\circ$  range at the ground station), and the position error of satellite is around  $10^{-2}$  m (Kang *et al.* 2006; Guo *et al.* 2015), which is the precision of current GPS satellite precise ephemeris. Satellite's velocity relative to ground is about  $3000 \text{ m s}^{-1}$ , with its accuracy better than  $10^{-3} \text{ m s}^{-1}$  (Remondi 2004; Zhang *et al.* 2006). The centrifugal acceleration of ground station  $|\vec{a}_e|$  is at most  $3.4 \times 10^{-2} \text{ m s}^{-2}$  (at the equator) (Pavlis *et al.* 2008). According to eq. (2), the error terms caused by position plus acceleration and velocity uncertainties are, respectively, expresses as

$$\frac{\Delta f_{\text{pos}}}{f_0} = \sqrt{\left( \frac{\Delta \vec{r}_{se} \cdot \vec{a}_e}{c^2} \right)^2 + \left( \frac{\vec{r}_{se} \cdot \Delta \vec{a}_e}{c^2} \right)^2} \quad (24)$$

$$\frac{\Delta f_{\text{vel}}}{f_0} = \frac{\Delta \vec{v}_{es} \cdot \vec{v}_{es}}{c^2} \quad (25)$$

where  $\Delta \vec{r}_{se}$  and  $\Delta \vec{v}_{es}$  are the position error and velocity error between ground station and spacecraft, respectively,  $\Delta \vec{a}_e$  is the centrifugal acceleration error of ground station. The Earth's angular velocity  $\omega$  is  $7.2921150 \times 10^{-5} \text{ rad s}^{-1}$ , with its relative uncertainty  $\Delta \omega = 1.4 \times 10^{-8}$  (Groten 2000). According to the centrifugal acceleration expression  $a = \omega^2 R_e$  (on equator), we can estimate the uncertainty of  $\vec{a}_e$  as

$$|\Delta \vec{a}_e| < 2\Delta \omega \cdot \omega \cdot R_e + \omega^2 \cdot \Delta R_e \quad (26)$$

where  $R_e$  and  $\Delta R_e$  are the Earth's equatorial average radius (6378136.6 m) and its uncertainty ( $1.5 \times 10^{-8}$ ) (Groten 2000). Then, from eq. (26) we have  $|\Delta \vec{a}_e| \leq 1.46 \times 10^{-9} \text{ m s}^{-2}$ , and based on eqs (24) and (25), we have

$$\Delta f_{\text{pos}}/f_0 \leq 3.57 \times 10^{-19}, \quad \Delta f_{\text{vel}}/f_0 = 3.33 \times 10^{-17}. \quad (27)$$

Eq. (21) provides the ionosphere shift effect, and the residual ionosphere error  $\Delta f_{\text{rion}}$  mainly comes from the error of electron density  $\rho$  in ionospheric electron density model, which is generally less than 20 per cent (Kang *et al.* 1997; Nava *et al.* 2008). Since the frequency  $f$  is set as  $f_0 = 2.0 \text{ GHz}$ , satellite's typical height above ground is  $H = 20000 \text{ km}$ , assuming the electron density  $\bar{\rho}$  being critical value  $5 \times 10^{11} \text{ m}^{-3}$  as a peak case (Bilitza *et al.* 2014), then we have

$$\frac{\Delta f_i}{f_0} = \frac{78570\bar{\rho}}{2cf_0^2} \cdot |\vec{a}_e| \cdot \Delta t \cdot \cos \alpha < 2.75 \times 10^{-18} \quad (28)$$

and the remaining ionospheric frequency shift error  $\Delta f_{\text{rion}}$  is smaller than the 20 per cent of  $\Delta f_i$  (Kang *et al.* 1997; Nava *et al.* 2008), namely

$$\frac{\Delta f_{\text{rion}}}{f_0} < 5.5 \times 10^{-19}. \quad (29)$$

We have also given the troposphere shift correction by eq. (22). According to Earth Global Reference Atmospheric Model (Leslie & Justus 2011), the values of  $\bar{M}_1$  and  $\bar{M}_2$  are  $1.8 \times 10^{-5}$  and  $2.0 \times 10^{-5}$ , respectively. Then, we have:

$$\frac{\Delta f_t}{f_0} = -\frac{60(\bar{M}_1 + \bar{M}_2)|\vec{r}_{se}|(\vec{v}_s - \vec{v}_e) \cdot \vec{a}_e}{c^2 H |\vec{v}_s - \vec{v}_e|} < 9.47 \times 10^{-19}. \quad (30)$$

According to eq. (30), the troposphere refraction effect in DCT is tiny (below the order of  $10^{-18}$ ) compared to other error sources, and it can be safely neglected without needing consideration.

The final term, random error  $\Delta f_{\text{ran}}$  comes from other high-order error sources, instrumental errors or system errors. For example, there would be a finite delay in the spacecraft transponder. Since the satellite is in motion, its position when receives signals are different from that when emits signals. Suppose we adopt a transponder (Pierro & Varasi 2013) that is designed for radio frequency (RF) signals, and the frequency  $f_0 = 2.0 \text{ GHz}$  is covered by the transponder's frequency range. The delay of the transponder is 800 ns (Pierro & Varasi 2013), thus the satellite moves only 0.24 mm between receiving and emitting signals and the satellite's direction of velocity changes  $2.53 \times 10^{-14} \text{ rad}$ . The absolute value of the satellite's velocity can be assumed to be unchanged during the 800 ns. Then, according to eqs (24) and (25), the errors caused by this position and velocity change are on the order of  $10^{-19}$ , which can be neglected. As explained in Section 2, the DCT method only involves frequency measurements; time delay does not need to be measured. Thus, the hardware time delays in both ground station and satellite can be neglected. In the short period of 800 ns, the signal's

frequency shift does not change, and since the stability of atomic clocks are assumed to be on the level of  $10^{-17}$ , we expect that the noises of frequency measurements are also on the level of  $10^{-17}$ . Thus, we only consider the satellite's position and velocity change in the error budget. Other error sources, such as measurement and data processing errors, can be reduced by multiple measurements and adjustment. We may expect this error term being controlled below  $1 \times 10^{-17}$ . Hence, the total error  $\Delta f_e/f_0$  is within the order of  $10^{-17}$ , namely

$$\begin{aligned} \frac{\Delta f_e}{f_0} &= \sqrt{\frac{\Delta f_{\text{osc}}^2 + \Delta f_{\text{pos}}^2 + \Delta f_{\text{vel}}^2 + \Delta f_{\text{rion}}^2 + \Delta f_{\text{rtro}}^2 + \Delta f_{\text{ran}}^2}{f_0^2}} \\ &\approx 10^{-17}. \end{aligned} \quad (31)$$

This study focuses on the general idea of determining the geopotential difference between a satellite/spacecraft and a ground station via radio links, closely related to the optical frequency of the OACs. The RF signal links are influenced by signal emission, transmission, reception and inevitable background noises (Rubiola 2005; Dawkins *et al.* 2007), which are referred to as instrument-induced errors. The influences due to the signal's propagation in free space are addressed as signal propagation errors. Concerning the error sources, here we concentrate on errors introduced by signal propagation in free space, leaving the instrument-induced errors to be dealt with in a separate paper, dedicated to instrumental techniques.

## 5 CONCLUSIONS

We formulated and discussed the gravitational frequency shift method for determining gravitational potential difference between a spacecraft (satellite) and a ground station. Based on this formulation, we may draw out gravitational frequency shift signals between a spacecraft and a ground station based on DCT. According to the general theory of relativity, the frequency shift of a light signal between a spacecraft and a ground station reflects the difference of the gravitational potential between them. Suppose atomic clocks with their inaccuracy of  $10^{-17}$  are available, our analysis shows that the uncertainty of the determined frequency shift by the approach proposed in this study can reach  $10^{-17}$ , which is equivalent to about  $1 \text{ m}^2 \text{ s}^{-2}$  in geopotential or 0.1 m in height determination. In the accuracy requirement in the level of  $10^{-17}$  as assumed in this study, we need not to consider the ionosphere and troposphere corrections, which are very small, around  $10^{-18}$ . However, for theoretical consideration and future ultrahigh precision requirement, we should take into account these corrections.

We used the characteristics of a GNSS satellite for error analysis. In fact any satellite/spacecraft is suitable for DCT, as long as it is visible at the ground station. Low-orbit satellites bear limitations when intended to serve as 'bridges' for the determination of geopotential differences between two ground sites that are separated by a long distance. For this purpose, a satellite ought to have a height of around 20 000 km (or larger) above the Earth's surface (like a GNSS satellite or a communication satellite). In practice, the worst case of two ground stations located on the opposite sides of the Earth, more 'bridges' (satellite network) might be needed. Alternatively, we may determine the geopotential difference between the mentioned two opposite ground stations via an intermediate ground station.

With quick development of time and frequency science and technology, the approach proposed in this study for determining the geopotential difference is prospective. The advantage of this

approach lies in that it is a very direct and convenient method to determine the orthometric height compared to the conventional levelling method. Based on this approach, besides the geometric position (coordinates) that can be precisely determined by well-known GNSS technique, the geopotential as well as orthometric height could be determined, realizing the determination of geometric position and orthometric height simultaneously. One of most prospective benefits from this approach is the realization of the world height system unification with centimetre level accuracy, once clocks with inaccuracy of  $10^{-18}$  are available.

## ACKNOWLEDGEMENTS

We sincerely thank four anonymous reviewers for their valuable comments, corrections and suggestions on the original manuscript, which greatly improved the manuscript. We also thank Editor Prof Joerg Renner for his valuable comments, suggestions and corrections to improve the final manuscript. This study is supported by National 973 Project China (grant nos 2013CB733301 and 2013CB733305), NSFC (grant nos 41210006, 41374022 and 41429401), DAAD (grant no. 57173947) and NASG Special Project Public Interest (grant no. 201512001).

## REFERENCES

- Altschul, B. *et al.*, 2014. Quantum tests of the Einstein Equivalence Principle with the STE-QUEST space mission, *Adv. Space Res.*, **55**(1), 501–524.
- Bilitza, D., Altadill, D., Zhang, Y., Mertens, C., Truhlik, V., Richards, P., McKinnell, L. & Reinisch, B., 2014. The International Reference Ionosphere 2012—a model of international collaboration, *J. Space Weather Space Clim.*, **4**, A07, doi:10.1051/swsc/2014004.
- Bjerhammar, A., 1985. On a relativistic geodesy, *Bull. Géod.*, **59**(3), 207–220.
- Bloom, B.J. *et al.*, 2014. An optical lattice clock with accuracy and stability at the 10<sup>-18</sup> level, *Nature*, **506**(7486), 71–75.
- Botter, T., Williams, J., Chiow, S.-W., Kellogg, J. & Yu, N., 2014. The development of atom-interferometry-based instruments for space missions, in *45th Annual Meeting of the APS Division of Atomic, Molecular and Optical Physics*, Vol. 59(8), P6.00004.
- Cohenour, C. & Frank, V.G., 2011. GPS orbit and clock error distributions, *Navigation*, **58**(1), 17–28.
- Dawkins, S.T., McFerran, J.J. & Luiten, A.N., 2007. Considerations on the measurement of the stability of oscillators with frequency counters, *IEEE Trans. Ultrason. Ferroelectr. Freq. Control*, **54**(5), 918–925.
- Einstein, A., 1915. Die feldgleichungen der gravitation, *Sitz.ber., König. Preuß. Akad. Wiss. (Berlin)*, **1**, 844–847.
- Groten, E., 2000. Parameters of common relevance of astronomy, geodesy, and geodynamics, *J. Geod.*, **74**(1), 134–140.
- Guo, J., Zhao, Q., Guo, X., Liu, X., Liu, J. & Zhou, Q., 2015. Quality assessment of onboard GPS receiver and its combination with DORIS and SLR for Haiyang 2A precise orbit determination, *Sci. China Earth Sci.*, **58**(1), 138–150.
- Hechenblaikner, G., Hess, M.P., Vitelli, M. & Beck, J., 2014. STE-QUEST mission and system design, *Exper. Astron.*, **37**(3), 481–501.
- Hinkley, N. *et al.*, 2013. An atomic clock with 10<sup>-18</sup> inaccuracy, *Science*, **341**(6151), 1215–1218.
- Hofmann-Wellenhof, B. & Moritz, H., 2006. *Physical Geodesy*, Springer Science & Business Media.
- Juan, J.M., Rius, A., Hernández, P.M. & Sanz, J., 1997. A two-layer model of the ionosphere using Global Positioning System data, *Geophys. Res. Lett.*, **24**(4), 393–396.
- Kang, Z., Tapley, B., Bettadpur, S., Ries, J., Nagel, P. & Pastor, R., 2006. Precise orbit determination for the GRACE mission using only GPS data, *J. Geod.*, **80**(6), 322–331.
- Leslie, F.W. & Justus, C.G., 2011. *The NASA Marshall Space Flight Center Earth Global Reference Atmospheric Model—2010 Version*, NASA/TM-2011-216467, NASA Marshall Space Flight Center.
- Levine, J., 2008. A review of time and frequency transfer methods, *Metrologia*, **45**(6), S162–S174.
- Millman, G.H. & Arabadjis, M.C., 1984. Tropospheric and ionospheric phase perturbations and doppler frequency shift effects, NASA Sti/recon Technical Report No., 85.
- Namazov, S.A., Novikov, V.D. & Khmel'nitskii, I.A., 1975. Doppler frequency shift during ionospheric propagation of decimeter radio waves (review), *Radiophys. Quantum Electron.*, **18**(4), 345–364.
- Nava, B., Coisson, P. & Radicella, S.M., 2008. A new version of the NeQuick ionosphere electron density model, *J. Atmos. Sol.-Terr. Phys.*, **70**(15), 1856–1862.
- Pail, R. *et al.*, 2011. First GOCE gravity field models derived by three different approaches, *J. Geod.*, **85**(11), 819–843.
- Pavlis, N.K., Holmes, S.A., Kenyon, S.C. & Factor, J.K., 2008. An earth gravitational model to degree 2160, in *Paper Presented at the 2008 General Assembly of the European Geosciences Union*, Vienna, Austria, April 13–18.
- Pierno, L. & Varasi, M., 2013. Switchable delays optical fibre transponder with optical generation of doppler shift, United States Patent 8466831 B2.
- Remondi, B., 2004. Computing satellite velocity using the broadcast ephemeris, *GPS Solut.*, **8**(3), 181–183.
- Rubiola, E., 2005. On the measurement of frequency and of its sample variance with high-resolution counters, *Rev. Sci. Instrum.*, **76**(5), 054703-1–054703-6.
- Schiller, S. *et al.*, 2012. The space optical clocks project: development of high-performance transportable and breadboard optical clocks and advanced subsystems, *Eur. Freq. Time Forum*, **48**(11), 412–418.
- Shen, W., Chao, D. & Jin, B., 1993. On relativistic geoid, *Boll. Geod. Sci. Aff.*, **52**(3), 207–216.
- Shen, W., Ning, J., Chao, D.B. & Liu, J.N., 2009. A proposal on the test of general relativity by clock transportation experiments, *Adv. Space Res.*, **43**(1), 164–166.
- Shen, W., Ning, J., Liu, J., Li, J. & Chao, D., 2011. Determination of the geopotential and orthometric height based on frequency shift equation, *Nat. Sci.*, **3**(5), 388–396.
- Smith, E.K. & Weintraub, S., 1953. The constants in the equation for atmospheric refractive index at radio frequencies, *Proc. IRE*, **41**(8), 1035–1037.
- Tapley, B.D., Srinivas, B., Ries, J.C., Thompson, P.F. & Watkins, M.M., 2004. GRACE measurements of mass variability in the Earth system, *Science*, **305**(5683), 503–505.
- Ushijima, I., Takamoto, M., Das, M., Ohkubo, T. & Katori, H., 2015. Cryogenic optical lattice clocks, *Nat. Photon.*, **9**(3), 185–189.
- Vessot, R. & Levine, M.W., 1979. A test of the equivalence principle using a space-borne clock, *Gen. Relativ. Gravit.*, **10**(3), 181–204.
- Westergaard, P.G., Lodewyck, J., Lorini, L., Lecallier, A., Burt, E., Zawada, M., Millo, J. & Lemonde, P., 2011. Lattice induced frequency shifts in Sr optical lattice clocks at the 10<sup>-17</sup> level, *Phys. Rev. Lett.*, **106**(21), 210801, doi:10.1103/PhysRevLett.106.210801.
- Zhang, K., Grenfell, R. & Zhang, J., 2006. GPS satellite velocity and acceleration determination using the broadcast ephemeris, *J. Navig.*, **59**(2), 293–306.